Aerosol and Air Quality Research, 14: 108–123, 2014

ISSN: 1680-8584 print / 2071-1409 online
doi: 10.4209/aaqr.2013.03.0079

Identification and Classification of Different Aerosol Types over a Subtropical Rural Site in Mpumalanga, South Africa: Seasonal Variations as Retrieved from the AERONET Sunphotometer

Kanike Raghavendra Kumar[1†*], Venkataraman Sivakumar[1], Rajuru Ramakrishna Reddy[2], Kotalo Rama Gopal[2], Ayodele Joseph Adesina[1]

[1] *Discipline of Physics, School of Chemistry and Physics, Westville Campus, University of KwaZulu–Natal, Durban 4000, KwaZulu-Natal, South Africa*
[2] *Department of Physics, Aerosol and Atmospheric Research Laboratory, Sri Krishnadevaraya University, Anantapur 515 003, Andhra Pradesh, India*

ABSTRACT

This paper reports the observational results of aerosol optical characteristics, modification processes and discrimination of key aerosol types over Skukuza (24.9°S, 31.5°E, and 150 m), a subtropical rural site in South Africa (SA), using CIMEL Sunphotometer data, part of the AErosol RObotic NETwork (AERONET), from December 2005 to November 2006. The results show that a pronounced spectral and temporal variability in the optical properties of aerosols is mainly due to anthropogenic emissions. The discrimination of different aerosol types over Skukuza is also made using the daily mean values of aerosol optical depth at 500 nm (AOD_{500}) and Ångström exponent ($\alpha_{440\text{-}870}$) by applying the threshold values. The results of the analysis indentified three individual components (biomass burning/urban (BU), desert dust (DD) and clean maritime (CM) aerosol types) of differing origin, composition and optical characteristics, and revealed that the percentage contribution of each of type of aerosol changed significantly from season to season. We also derived the curvature of a_2 in an attempt to obtain information on aerosol-particle size and type, although the results revealed that the curvature alone is not enough to achieve this. In addition,, we analyzed the seasonal changes in aerosol characteristics using the classification scheme introduced in Gobbi *et al.* (2007) based on the measured scattering properties (α, $d\alpha$) derived from the Sunphotometer data. The results show that during spring an extremely large fraction of fine-mode aerosols ($\eta > 70\%$, $R_f \sim 0.1$ μm) in the turbid atmosphere was mainly caused by local anthropogenic pollution or biomass aerosol transported from forest fires. Whereas in summer, the low AOD (< 0.2) and smaller α (< 1.0) and $\eta < 50\%$ suggest the influence of transported mineral dust (coarse) over the region.

Keywords: AERONET; Skukuza; Optical properties; Aerosol types; Curvature.

INTRODUCTION

Atmospheric aerosols are solid or liquid particles suspended in the air. They have significance at local, regional and global scales and have received prominent attention in the past few years (Penner *et al.*, 1994; Seinfeld and Pandis, 2006). The climatic and environmental effects of atmospheric aerosols are the critical issues in global science community because aerosols, derived from natural and anthropogenic emission sources, are well known to affect the air quality, human health, and radiation budget (IPCC, 2007, Srivastava *et al.*, 2012). Uncertainty in quantifying the climatic impacts of aerosols continues to be greater than that of greenhouse gases (IPCC, 2007) due to variety of their sources, varying trends in aerosol loading and extreme heterogeneity in the spatial and temporal variability of their optical and microphysical properties (Morgan *et al.*, 2006; Kaskaoutis *et al.*, 2010). Therefore, the accurate assessment of the aerosol impact on radiative transfer is a complex task, since various aerosol types cause different effects on the solar radiation spectral distribution (Kaskaoutis and Kambezidis, 2008). Thus, detailed knowledge of the optical properties of the key aerosol types is highly essential. Numerous studies

† Now at Key Laboratory for Aerosol-Cloud-Precipitation of China Meteorological Administration, School of Atmospheric Physics, Nanjing University of Information Science and Technology, Nanjing 210044, Jiangsu, China.

* Corresponding author.
Tel.: +27 31 2601430
E-mail address: kanike.kumar@gmail.com

have been undertaken to characterize the aerosol properties at several worldwide locations (Piketh *et al.*, 1999; Dubovik *et al.*, 2002; Pace *et al.*, 2006; Kaskaoutis *et al.*, 2007a, b; El-Metwally *et al.*, 2008; Ogunjobi *et al.*, 2008; Kanike *et al.*, 2012).

South Africa (SA) extended between the latitudes 22°S–36°S and longitudes 16°E–34°E, is part of southern hemispheres subtropical zone comprising of provinces Limpopo, Mpumalanga, North West, KwaZulu-Natal, Free State and Gauteng (see Fig. 1) is among the areas with high aerosol concentrations compared to rest of the provinces in SA, as a result of recent rapid urbanization and population growth. The increase in aerosols potentially has significant impacts on regional climate and air quality (Formenti *et al.*, 2002; Freiman and Piketh. 2003; Sivakumar *et al.*, 2010; Kumar *et al*., 2013a). The SA region has been recognized as a major source of aerosols in the southern hemisphere and it is known to be significant in the production and transportation of aerosols with urban and industrial areas as major sources (Siversten *et al.*, 1995; Piketh *et al.*, 1999). Besides these, emissions from biomass burning also contribute relatively significant fraction to the total aerosol loading and is also impacted by airmasses associated with anthropogenic and natural sources, making the region an aerosol hotspot (Piketh *et al.*, 1999; Eck *et al.*, 2001b, 2003a; Queface *et al.*, 2011; Tesfaye *et al.*, 2011; Kumar *et al.*, 2013a, b).

The wavelength dependence of aerosol optical depth (AOD), commonly expressed by Ångström exponent, α (Ångström, 1964), varies between different aerosol types because of their different physical and chemical characteristics. The derivation of α in different wavelength bands is a useful tool for distinguishing and characterizing the aerosol type (Eck *et al.*, 1999; Schuster *et al.*, 2006). Recently, Gobbi *et al.* (2007) introduced a straight-forward graphical frame-work that allows discriminating different aerosol types based on aerosol spectral measurements by Sunphotometer which can be characterized by three independent pieces of information: AOD, α and the spectral curvature of α (dα). Plotting data in this space allow for inference of the aerosol fine mode size and fractional contribution to total AOD. The curvature a_2 (second-order polynomial fit to ln(AOD) versus ln(λ)) can be utilized in conjunction with the AOD for the discrimination of the different aerosol types, and can also be used as an indicator of the relative influence of fine- versus coarse-mode particles in the aerosol size (Eck *et al.*, 1999; Schuster *et al.*, 2006). Hence the information of AOD, α and spectral curvature can be used in identifying the type of aerosols.

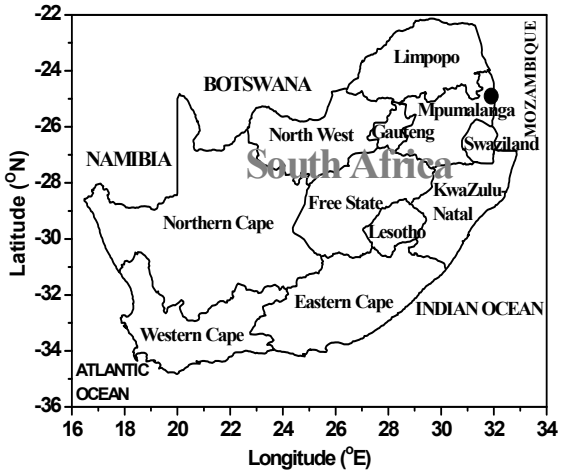

Fig. 1. Geographical map of South Africa with the positioning of the measurement site, Skukuza represented with black solid circle denoted with all its provinces, boundaries, and surroundings oceans.

Several earlier researchers, to name a few, Dubovik *et al.* (2002), Eck *et al.* (2003a), and Queface *et al.* (2011) reported that biomass burning aerosols dominate other aerosol types and peaks during the dry season over Skukuza (latitude: 24°59'S; longitude: 31°35'E; elevation: 150 m), a subtropical rural station in Mpumalanga province of South Africa (see Fig. 1) using the data obtained from AErosol RObotic NETwork (AERONET) Sunphotometer. More recently, Kumar *et al.* (2013b) also observed that the AOD over Skukuza varies with season and is mainly influenced by biomass burning with a minor contribution of sea-salt, desert dust and urban-industrial aerosols. This study was limited to monthly/ seasonal patterns of aerosols optical properties, the AOD-α relationship, influence of meteorology and long range transport of airmass pathways. The above same authors (Kumar *et al.*, 2013b) interested to expand their previously reported work here by investigating in detail about the different aerosol types prevailing over Skukuza, making use of the same AOD and α data derived from the AERONET Sunphotometer. In the present study, we examine the changes in the aerosol optical characteristics making use of the classification (graphical) scheme proposed by Gobbi *et al.* (2007), discrimination of aerosol types, effect of curvature on each aerosol type, and its relationship with the AOD and the Ångström exponent and their seasonal distinctiveness. In section 2, we describe the selected geographical site and the method applied for the analysis of data used from Skukuza AERONET site, while in section 3 the analysis of the results obtained are presented. Finally, the main conclusions drawn from the present work are mentioned in section 4.

EXPERIMENTAL SITE AND METEOROLOGY

Site Description

The observation site, Skukuza (24°59'S; 31°35'E, 150 m), which is a subtropical region located in the Kruger National Park in the northeastern part of a fast growing urban province, Mpumalanga in South Africa (Kumar *et al.*, 2013). With its ~3.8 million inhabitants, Mpumalanga is the second smallest province after Gauteng, taking up 6.5% of South Africa's land area. This is a direct result of the growth in population, industrial emissions and also associated activities that have been observed during the last decades. In addition to this, particles produced by seasonal sources can be transported towards the study region at certain times of the year. This is the case of mineral dust produced mainly in summer, though not extensively, and

the biomass burning of the sugar cane crop residues as well as forest fires because of its dense grassland areas in the dry (spring) period (Piketh *et al.*, 1999). The measurement site also experiences smoke generated from the coal-fired power stations, which are the biggest in the southern hemisphere. Because of its potential effects on people's health, the persistence of high levels of particulate matter concentrations and biomass/smoke particles over Skukuza is a matter of great concern for its inhabitants.

Meteorology

More details about the study region, prevailing atmospheric circulations derived from NCEP/NCAR reanalysis, local meteorological data provided by South African Weather Services (SAWS) and effect of aerosol properties through long range transport from different types of airmasses over the measurement location using HYSPLIT model are described recently by the same authors reported by Kumar *et al.* (2013b) for the same measurement period over Skukuza and are not given herein to avoid repetition.

MEASUREMENTS AND METHODOLOGY

AERONET Instrumentation

The measurements used in this work have been obtained from the CIMEL Sunphotometer (CE-318) of AERONET working group, which is an automatic sun-sky scanning spectral radiometer. A brief description is given here since a number of studies have already described the instrumentation, data acquisition, retrieval algorithms and calibration procedures, which confirm to the standard of the AERONET global networks, as well as the uncertainty of the final products and the applied cloud-screening procedures (Holben *et al.*, 1998; Eck *et al.*, 1999; Smirnov *et al.*, 2000; Holben *et al.*, 2001; Smirnov *et al.*, 2002a, b). The AERONET data were provided in three categories: cloud-contaminated (level 1.0), cloud-screened (level 1.5), following the methodology described by Smirnov *et al.* (2000), and cloud-screened and quality-assured (level 2.0), which have been used in the present study. The Sunphotometer takes measurements of the direct-beam radiances within the spectral range 340-1020 nm. Typically, the total uncertainty in spectral AOD is about ± 0.01 to ± 0.02, and is spectrally dependent with the higher errors in the UV band (Srivastava *et al.*, 2012). The calibration accuracy becomes an obstacle because it causes an error in measuring AOD (± 0.01) that is at least of the order of 5–10% of the calculated optical depth for $AOD_{440} < 0.2$, and comparable with the absorption partition in the total optical depth (Dubovik *et al.*, 2002).

From the AERONET data, a single Ångström wavelength exponent, α, is derived in the 440–870 nm band from the linear regression of ln(AOD) versus ln(λ) with data obtained at four wavelengths using the least-squares method, while λ stands for the wavelength in μm. Furthermore, the linear fit that is used for the calculation of α in a log-log plot exhibits some uncertainties due to the curvature of AOD with respect to wavelength (Eck *et al.*, 1999).

Method of Data Analysis

The spectral dependence of AOD is used in this work to compute the Ångström's exponent α. A spectrally-averaged value of this exponent, which contains information about size of the particles or the volume fraction of the fine- versus coarse-mode particles (Schuster *et al.*, 2006), can be obtained by fitting the Ångström's formula (Ångström, 1964)

$$AOD_\lambda = \beta\lambda^{-\alpha} \quad (1)$$

where AOD_λ is the estimated AOD at the wavelength λ, β is the Ångström's turbidity coefficient, which equals AOD at λ = 1 μm, and α is the Ångström exponent. Although in this definition, α is assumed independent from the wavelength, it is established that the opposite exist. (e.g., Kaskaoutis and Kambezidis, 2008). The Ångström formula is a special case of a more complicated equation valid for a limited range of particle diameters and a limited interval of wavelengths. The validity of this theory presupposes that the Junge power law is valid for the particle radius range, where significant extinction takes place and that the spectral variation of the refractive index does not impose significant variations on the Mie extinction factor (Kaskaoutis *et al.*, 2007b). Taking the logarithms on both sides of Eq. (1) one obtains

$$\ln AOD_\lambda = -\alpha \ln\lambda + \ln\beta \quad (2)$$

A more precise empirical relationship between aerosol extinction and wavelengths is obtained with a second-order polynomial approximation (King and Byrne, 1976; Eck *et al.*, 1999; Pedros *et al.*, 2003; Kaskaoutis and Kambezidis, 2006),

$$\ln AOD_\lambda = a_2 (\ln\lambda)^2 + a_1 \ln\lambda + a_0 \quad (3)$$

where the coefficient a_2 account for the spectral curvature of the fitted function. This curvature can be an indicator of the aerosol particle size; negative curvature indicates aerosol-size dominated by fine-mode and positive curvature with significant contributions from coarse-mode aerosols (Eck *et al.*, 1999; Reid *et al.*, 1999; Schuster *et al.*, 2006). In the present study, the values of Ångström exponent α were computed in the wavelength interval 440–870 nm, applying the least squares method to Eq. (2). Choice of the 440–870 nm wavelength range relies on the fact that these are highly accurate channels of the Sunphotometer (Holben *et al.*, 1998; Eck *et al.*, 1999) and these channels are available in all AERONET group instruments. The liner fit to the logarithmic function of Eq. (2) is the most precise method, although the results may also depend on the spectral interval considered (Pedros *et al.*, 2003). The second order polynomial fit (Eq. (3)) was also applied to the AOD values at six wavelengths (340, 380, 440, 500, 675, and 870 nm). Although the polynomial fit to Eq. (3) is more precise than the linear fit to Eq. (2), large errors can appear especially under low turbidity conditions (Kaskaoutis *et al.*, 2006). For limiting these errors, only the case where the second-order polynomial fit was associated with $R^2 > 0.95$ were considered. It should be noted that the AOD_{1020} values were omitted from the fits, since it contain larger uncertainties due to the water

vapor effect.

Discrimination of Aerosol Types

When attempting a realistic characterization of the aerosol properties, data of both AOD and α have to be used (Holben *et al.*, 2001) since they both strongly depend on wavelength. Thus scatterplots of AOD versus α can be obtained in order to determine the different aerosol types for a specific location through the discrimination of physically interpretable cluster regions represented in a diagram (Cachorro *et al.*, 2001; Pace *et al.*, 2006; Kaskaoutis *et al.*, 2007a). These AOD-α patterns have been observed at several locations and for different aerosol types (e.g., biomass smoke, anthropogenic aerosols, desert dust) (Eck *et al.*, 1999, 2001, 2003a, b; Masmoudi *et al.*, 2003; Kim *et al.*, 2004; Ogunjobi *et al.*, 2004). This method has been used in a number of studies (for example, Kalapureddy *et al.*, 2009; Kaskaoutis *et al.*, 2009, and references therein) and is based on the sensitivity of the two parameters to different, somewhat independent, microphysical aerosol properties; the Ångström exponent, α depends on aerosol particle size, while the AOD_{500} depends mainly on the aerosol column density. Therefore, the AOD_{500} versus $\alpha_{440\text{-}870}$ plot qualitatively indicates the amount and dimension of the observed aerosols.

In the present study, the contour maps were constructed using 0.1 and 0.2 steps for both AOD_{500} and $\alpha_{440\text{-}870}$ values, respectively. In these maps, the rectangle areas denote different aerosol types, namely, clean maritime (CM), biomass burning/urban-industrial (BU), desert dust (DD), and mixed type (MT) aerosols, and boundaries of these areas correspond to the selected threshold value of AOD_{500} and $\alpha_{440\text{-}870}$. In such studies, the selection of the threshold values can be very important. In the present study, the AOD_{500} ranges from 0.01 to 0.7 and the $\alpha_{440\text{-}870}$ spans between 0.1 and 3.0. Therefore, the threshold values must be slightly changes from those utilized by Pace *et al.* (2006) for Lampedusa. Therefore, (i) values of $AOD_{500} < 0.07$ with $\alpha_{440\text{-}870}$ values < 1.5 represent clean maritime (CM) aerosols, (ii) $AOD_{500} > 0.1$ and $\alpha_{440\text{-}870} > 1.3$ can be used to characterize long-range transported biomass burning/urban-industrial (BU) aerosols, and (iii) AOD_{500} values > 0.15 associated with $\alpha_{440\text{-}870} < 0.7$ are indicative of desert dust (DD) particles transported over oceanic areas. Finally, the remaining gaps reveal where the aerosols are difficult to be discriminated and they are considered as mixed type (MT) aerosols, bearing in mind the different effects of various aerosol-mixing processes in the atmosphere (e.g., coagulation, condensation, humidification, gas-to-particle conversion).

Aerosol Modification Processes

Aerosol spectral measurements can be characterized by three independent variables: (i) the AOD, (ii) the Ångström exponent (α), and (iii) the spectral curvature of α (dα). In this study, we discriminate the fraction of AOD due to large mineral particles from other aerosol types, based on the graphical framework introduced in Gobbi *et al.* (2007) (see Fig. 1 of Gobbi *et al.* (2007)) which allows to: 1) infer aerosol fine mode size and fractional contribution to the total AOD; and 2) separate AOD increases due to fine-mode aerosol humidification from AOD increases due to the increase in coarse particles. The method relies on the combined analysis of α derived for the wavelength pairs of 440–870 nm and its spectral curvature, represented by $d\alpha = \alpha(440, 675) - \alpha(675, 870)$. For the definition of these coordinates (dα vs. α space), reference points corresponding to biomodal size distributions characterized by a fine-mode modal radii (R_f) as well as the ratio of fine-mode to total AOD (η) have been determined on the basis of typical refractive index of urban/industrial aerosol (m = 1.4 – 0.001i). Varying coarse-mode modal radii (R_c) have been considered and shown to have a minor modal radii on such reference points. Gobbi *et al.* (2007) showed the sensitivity of the classification scheme to refractive index. Computations indicated some clockwise rotation about the origin of the constant radius curves for increasing refractive index, while the effect is much weaker in the case of η. Maximum R_f indetermination is of the order of ± 25% for refractive index varying between m = 1.33 – 0.0i and m = 1.53 – 0.003i, while the η spans a range of the order of ±10 %. Within this level of indetermination, the scheme is robust enough to provide an operational classification of the aerosol properties.

In this α vs. dα space, we represent AOD (at 675 nm) by a color scale. The correlation of α vs. dα plot with the fine-mode fraction to the AOD at 675 nm (η) and effective radius of fine aerosols (R_f) is appropriate for identifying aerosol-modification processes, i.e., cloud contamination, hydration, and coagulation-aging. The same scheme was performed over Skukuza (South Africa), a subtropical rural site, with the initiation of earlier researchers (Gobbi *et al.*, 2007; Basart *et al.*, 2009) who reported in their work to explore information about aerosol types over this site. Recently, it has been applied over oceanic environment during ICARB in summer (Arabian Sea) (Kaskaoutis *et al.*, 2010), W-ICARB in winter (Bay of Bengal) (Kaskaoutis *et al.*, 2011), while over different urban environments of Athens by means of MFR data (Gerasopoulos *et al.*, 2011) and over Hyderabad from MICROTOPS II Sunphotometer observations (Sinha *et al.*, 2012). Gobbi *et al.* (2007) used only cases of AOD > 0.15 from eight different AERONET stations in three continents to avoid errors larger than ~30%. In the present study also, the whole set of observations (only AOD > 0.1) was used in order to avoid errors and reveal any systematic uncertainties.

RESULTS AND DISCUSSION

In the present work, we have classified the data in terms of four major seasons, namely, summer (December–February), autumn (March–May), winter (June–August) and spring (September–November) seasons, primarily on the basis of synoptic winds and different meteorological conditions prevailing over this site (Queface *et al.*, 2011; Kumar *et al.*, 2013b).

Spectral Variation of AOD and Identification of Aerosol Types

Spectral AOD is a key parameter in estimating the extent to which aerosols directly influence the radiative balance

of the earth-atmosphere system and is dependent on the columnar abundance, size distribution and refractive index of aerosols. The spectral variation of AOD ($\tau_{p\lambda}$) is important as it is an indicative of the changes in aerosol-size characteristics. Except for the rainy days, the weather is dry with abundant sunshine; however, cloud cover is frequently seen throughout the year. Because of this, measurements are scarce and we have only 261 days of observations during the entire study period (Kumar *et al.*, 2013b), which were grouped according to the seasons. The mean spectral distribution of AOD with respective standard deviation (vertical bars) observed in different seasons is shown in Fig. 2. A decrease of AOD with increase in wavelength is observed, which is consistent with the Mie theory (Kumar *et al.*, 2009). High AOD values observed at 340 nm suggest dominance of fine-mode particles over the study area. It is evident from the figure that there is relatively strong wavelength dependence of optical depth at shorter wavelengths that gradually decreases towards longer wavelengths irrespective of the seasonal change, attributing to the presence of fine to coarse particles. The presence of a higher concentration of the fine-mode particles which are selective scatters enhances the irradiance scattering, and therefore, the AOD values are high at the shorter wavelengths (Rana *et al.*, 2009). Likewise, the coarse-mode particles provide similar contributions to the AOD at both wavelengths (Schuster *et al.*, 2006). Fig. 2 also clearly depicts that the trend in the AOD pattern is almost similar in all the seasons with higher (lower) magnitudes in spring (autumn) season, with a mean value of 0.30 ± 0.14 (0.13 ± 0.11) at 500 nm (see Table 1). The observed increase in AOD_{500} during the spring season might be due to the local pronounced biomass burning activities in the northeastern and eastern part of SA as reported by Tesfaye *et al.* (2011) and Kumar *et al.* (2013) for the same study region. On the other hand, high AODs during the spring season could be attributed to the high convective activity and strong seasonal surface winds (see Table 1 and Fig. SI-1of Kumar *et al.*, 2013b), with a minor contribution by long range transported biomass burning and desert dust aerosols (Formenti *et al.*, 2002). A decrease in AOD values has been observed during autumn period due to cloud scavenging and rain-washout process (Moorthy *et al.*, 2005; Kaskaoutis *et al.*, 2009).

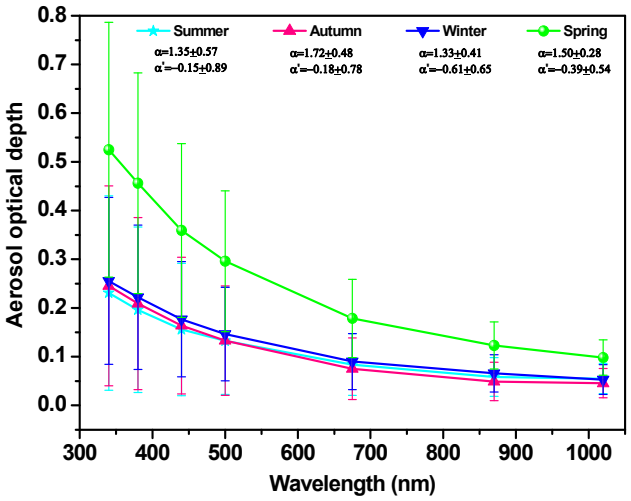

Fig. 2. Spectral characteristics of AOD for different seasons over Skukuza during the study period. Mean values of α and α' are also given for each season.

Table 1. Monthly average AOD_{500}, $\alpha_{440\text{-}870}$ and curvature (a_2) along with standard deviations observed over Skukuza for the study period.

Month	AOD_{500}	$\alpha_{440\text{-}870}$	a_2
December-05	0.14 ± 0.07	1.40 ± 0.46	0.20 ± 0.06
January-06	0.16 ± 0.15	1.26 ± 0.60	–0.02 ± 0.01
February-06	0.10 ± 0.10	1.37 ± 0.62	0.04 ± 0.02
March-06	0.12 ± 0.09	1.61 ± 0.59	0.18 ± 0.08
April-06	0.15 ± 0.12	1.82 ± 0.41	0.03 ± 0.09
May-06	0.13 ± 0.11	1.75 ± 0.43	0.07 ± 0.07
June-06	0.14 ± 0.09	1.44 ± 0.44	0.15 ± 0.06
July-06	0.15 ± 0.10	1.38 ± 0.40	0.32 ± 0.07
August-06	0.14 ± 0.09	1.18 ± 0.40	0.44 ± 0.05
September-06	0.21 ± 0.12	1.42 ± 0.25	0.28 ± 0.05
October-06	0.28 ± 0.14	1.42 ± 0.37	0.19 ± 0.05
November-06	0.39 ± 0.16	1.65 ± 0.21	0.09 ± 0.07

Fig. 3 depicts the density plots of AOD_{500} versus Ångström exponent ($\alpha_{440\text{-}870}$) over the Skukuza region for the four representative seasons. Viewing the contour density plot, some areas of larger density are observed representative of different aerosol types depend upon season. In the summer season which is characterized by relatively higher AOD_{500} and moderate $\alpha_{440\text{-}870}$ values (Fig. 3(a)). The different aerosol sources have a direct effect on the wide range of $\alpha_{440\text{-}870}$ values, from ~0.7 to ~1.7, especially for low AOD_{500} (< 0.3), suggesting variety of aerosol types. However, for smaller AOD_{500} the $\alpha_{440\text{-}870}$ increases to values higher than 1.0, assigning an increasing trend of the AOD_{500} versus $\alpha_{440\text{-}870}$ relationship. In the autumn, the $\alpha_{440\text{-}870}$ values are significantly higher (>2.0) than in the previous case with lower AOD_{500} (< 0.2) (see Fig. 3(b)). The maximum density area is observed for the pair (AOD_{500}, $\alpha_{440\text{-}870}$) = (0.05–0.2, 2.0–2.15) indicative of low turbid conditions with a rather mixed aerosol field in the vertical. The $\alpha_{440\text{-}870}$ values of this magnitude are indicative of bimodal aerosol size distributions, with significant contribution from both fine-mode (submicron, radius < 1 μm) and coarse-mode (supermicron, radius > 1 μm) aerosols (Eck *et al.*, 2005). In the winter season (Fig. 3(c)), the summer maximum seems to shift into three; one with AOD_{500} = 0.15–0.25 and $\alpha_{440\text{-}870}$ = 1.57–1.65 with larger fraction of fine-mode particles, a second with AOD_{500} = 0.1 and $\alpha_{440\text{-}870}$ = 1.4 corresponding to aerosols with anthropogenic or biomass burning origin probably, and a third with AOD_{500} = 0.07–0.15 and $\alpha_{440\text{-}870}$ = 1.0–1.15 dominance with coarse-mode particles under turbid conditions. The spring season (see Fig. 3(d)) is characterized by higher AOD_{500} (0.30 ± 0.14) and moderate $\alpha_{440\text{-}870}$ values (1.50 ± 0.28). The maximum density area of AOD_{500} = 0.2–0.4 and $\alpha_{440\text{-}870}$ = 1.5–1.7 is representative of the biomass burning aerosols from long-range transport which is frequent over the South Africa (Queface *et al.*, 2011; Tesfaye *et al.*, 2011; Kumar *et al.*, 2013b) during this season and relative

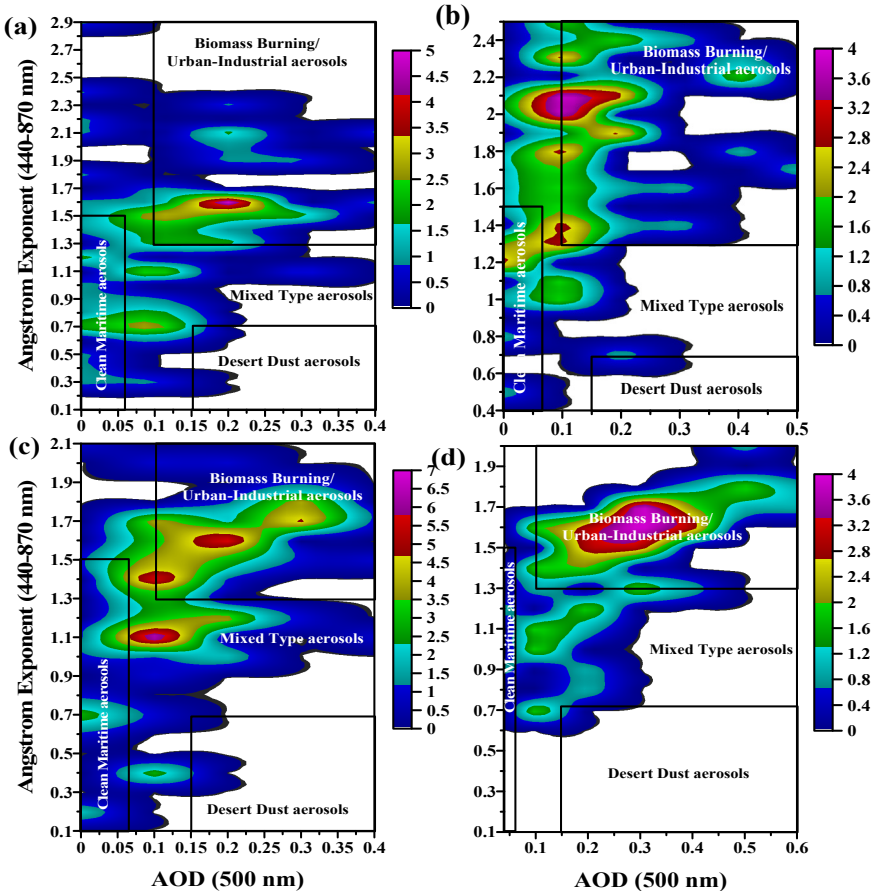

Fig. 3. Contour density maps of the AOD_{500} versus $\alpha_{440\text{-}870}$ relation in the (a) summer (b) autumn (c) winter and (d) spring seasons for the study period derived from CIMEL Sunphotometer.

influence of urban-industrial polluted aerosols under moderate-to-high turbid conditions. The other AOD_{500} and $\alpha_{440\text{-}870}$ pairs are nearly equally distributed around this area with preferable of larger AOD_{500}. The values of α depend strongly on the spectral range used for their determination. Hence the information contained in the AOD_{500} versus $\alpha_{440\text{-}870}$ scatterplot becomes more difficult to interpret, but the detailed spectral information given by the determination of α in different spectral band helps in determining and discriminating the aerosol types (Vijayakumar *et al.*, 2012).

Analysis of Different Aerosol Types

Fig. 4 shows the percentage contribution of each of the four different aerosol types noticed over Skukuza, based on the present AOD_{500} and $\alpha_{440\text{-}870}$ threshold values. The respective influences of the two aerosol types (CM and BU) are more balanced in winter and summer than during autumn and spring periods, when the % contribution of the specific aerosol types is larger. The contribution of aerosols of different origin and characteristics to the atmospheric column can be strongly modified in each season. The biomass burning/urban-industrial aerosol (BU) is predominant in all seasons, exhibits its higher frequency in spring (67.31%). The mixed type (MT) aerosol occupies next to BU in all seasons; with almost equal percentage of contribution of MT aerosol during the summer (26.67%) and winter (28.92%) seasons, with its maximum frequency in autumn (33.33%). Next to MT, the clean maritime (CM) aerosols are contributing more to the total loading in all the seasons, with its minimum in spring (3.85%) and almost equal % of share in summer (28.33%) and winter (26.51%). Thus, 28.33% of the CM aerosols are observed in summer, 28.92% of the MT aerosols in winter, 1.92% of DD aerosols in spring and 46.97% of BU aerosols in autumn periods. Quite interesting characteristics are the low percentage of CM aerosols observed in spring (3.85%, refer Fig. 4(d)), taking into account that the anthropogenic emissions are more significant compared to natural aerosols at Skukuza throughout the year. This can partly be explained by a quick modification of the produced water-soluble local aerosols that can enlarge in size due to humidification especially under the influence of the large relative humidity (RH) values in the summer/autumn seasons. Also, the transport of dust emissions from local sources and nearby deserts play a significant role in these seasons and the possible adhering of fine-mode pollution particles onto the surface of coarse-mode dust in the mixed aerosol (Kaskaoutis *et al.*, 2009). Since the majority of the aerosols belong to a BU aerosol type more attention must be paid to this type, as a result of independent processes. Thus, the mixing could be caused by primary small and large particles. The larger RH values closely associated with the lower $\alpha_{440\text{-}870}$ in autumn may be

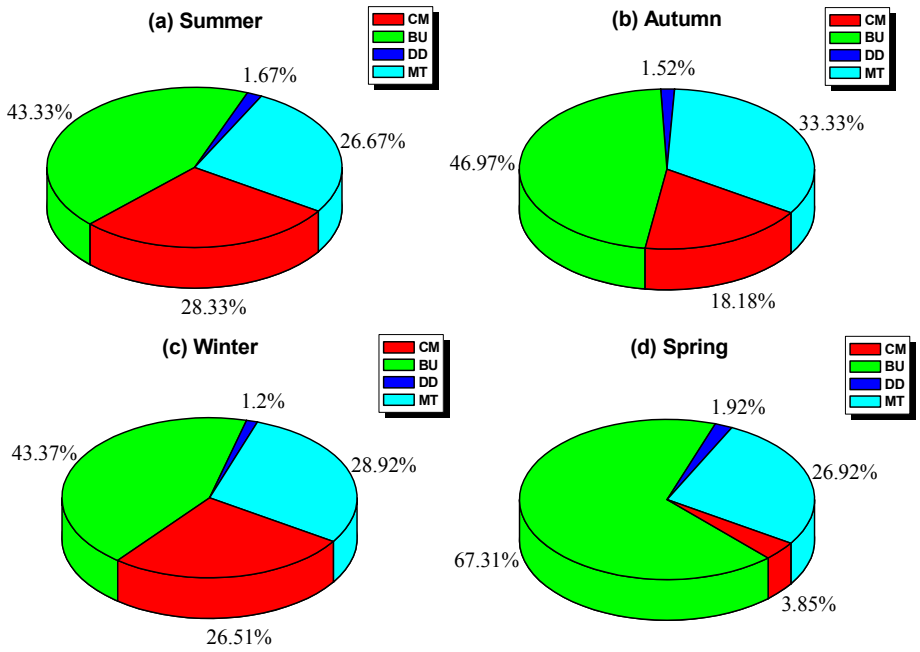

Fig. 4. Percentage of each aerosol type over Skukuza contributing to the total in each season during the study period. Labels stand as CM, clean maritime; BU, biomass burning/urban-industrial; DD, desert dust, and MT, mixed type.

an evidence of coagulation and hygroscopic growth of the water-soluble urban aerosols, since the higher growth factor includes the hygroscopic and water-soluble particles (Day and Malm, 2001). However, there is no detailed analysis in the present study to warrant it and further investigation is needed. Also, the possible cloud contamination in some cases in the autumn period results in lower $\alpha_{440\text{-}870}$, which associated with the high AODs, concludes to the CM type aerosols. On the other hand, the coarse-mode particles transported over Skukuza can easily be mixed with local pollution or with smoke from forest fires, increasing the wavelength dependence of AOD (Queface *et al.*, 2011).

Frequency of Occurrence in AOD_{500} and $\alpha_{440\text{-}870}$ Based on Aerosol Types

Fig. 5 shows the frequency distribution of AOD_{500} for the four aerosol types in different seasons. Such a figure reveals how AOD_{500} alone can give information about the discrimination of the aerosol types. Because of initial definition, the moderate CM aerosols are observed at lower AOD_{500} values (< 0.15), whereas, at higher AOD_{500} a biomass burning/urban-industrial (BU) aerosols predominance is clear from the discussion presented in the previous section; at moderate values of AOD_{500} (> 0.15) the DD aerosols have a minor negligible fraction and MT aerosols have significant contribution in all seasons. The CM, DD, and BU types are hardly distinguishable based on the AOD_{500} distribution; thus it is difficult to resolve them separately, especially in the moderate AOD_{500} values. The summer and autumn distributions present some similarities, despite the higher frequency of the BU aerosols in autumn, while in spring there is a clear discrimination between BU and DD aerosols, with the former distributed for a wide range to dominate for higher AOD_{500} > 0.3. In all the seasons, the BU type of aerosols has it maximum frequency it is found that all these cases correspond to biomass burning activities, characterized by large aerosol loading transported from sub-tropical zones of SA towards the measurement site. These BU aerosols can be mixed up with aerosols of other (mainly natural) origin, a process that often modifies their initial optical properties. AOD_{500} maxima can then be associated either with urban-industrial pollution and mixed aerosols or to a lesser extent, with dust particles. Large distribution of MT aerosols is observed for AOD_{500} > 0.05, where BU, CM and DD aerosols can be found only in winter and spring.

Similarly, Fig. 6 shows the frequency distribution of the aerosol types with respect to $\alpha_{440\text{-}870}$. In the scale of $\alpha_{440\text{-}870}$, the CM and DD aerosols are expected to fall in the lower end of $\alpha_{440\text{-}870}$ values, since both types are characterized by coarse-mode particles. It is surprising to note that all the aerosol types are absent for $\alpha_{440\text{-}870}$ values lower than 0.5 in spring. Note that the larger possibility of observing CM and DD aerosol types at lower $\alpha_{440\text{-}870}$ in spring with smaller occurrence than in the rest of the year shows that the importance of the biomass burning or mineral component is generally greater in this season. The CM type aerosol plays a significant role in the distribution of the $\alpha_{440\text{-}870}$ values in all the seasons except in spring with its minimum occurrence, since this is the dominant type for a wide range of $\alpha_{440\text{-}870}$ values (0.1–1.5), hindering the discrimination of the other aerosol types. This shows that the CM aerosol which mainly comprise of coarse-mode particles attributed to strong sea-salt production and has significant importance. For intermediate $\alpha_{440\text{-}870}$ values MT clearly dominates, while for $\alpha_{440\text{-}870}$ values above 1.0, BU and MT present strong and almost similar distribution pattern implying a difficulty in distinguishing them. In contrast, for low $\alpha_{440\text{-}870}$ values (< 1.0) the DD type cannot be distinguished from CM aerosol type,

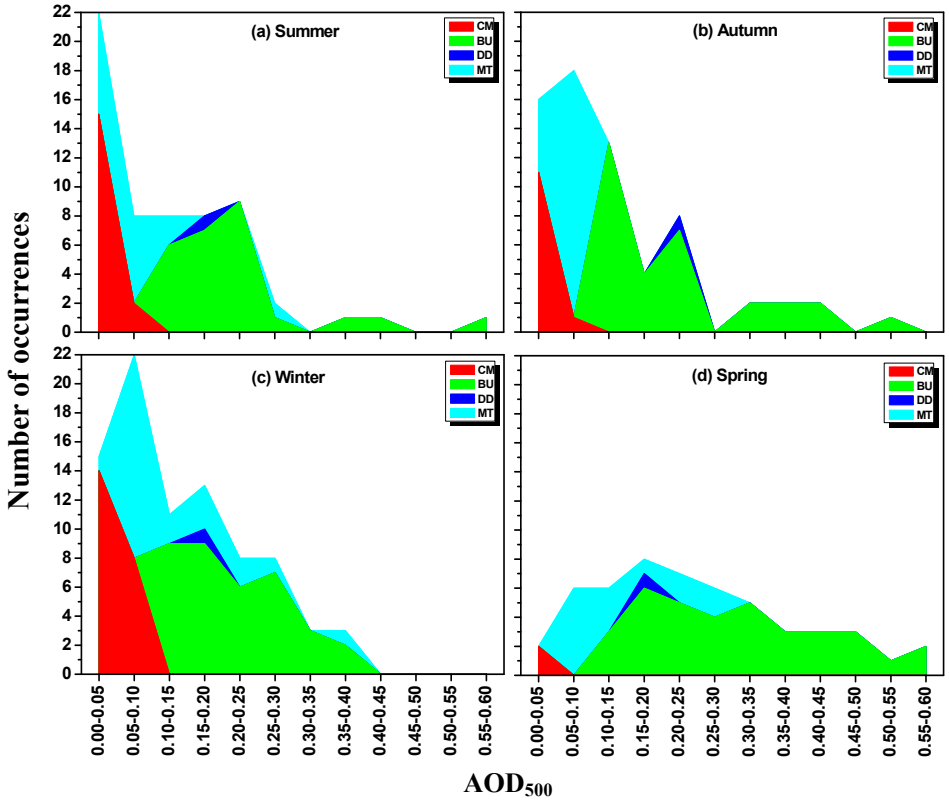

Fig. 5. Number of AOD_{500} values in various AOD_{500} intervals for the four aerosol types over Skukuza during the study period. The individual colors indicates differential number of occurrences corresponding to different aerosol types in each AOD_{500} interval, and the outer boundary represents the total number of occurrences for all the aerosol types in each AOD_{500} interval.

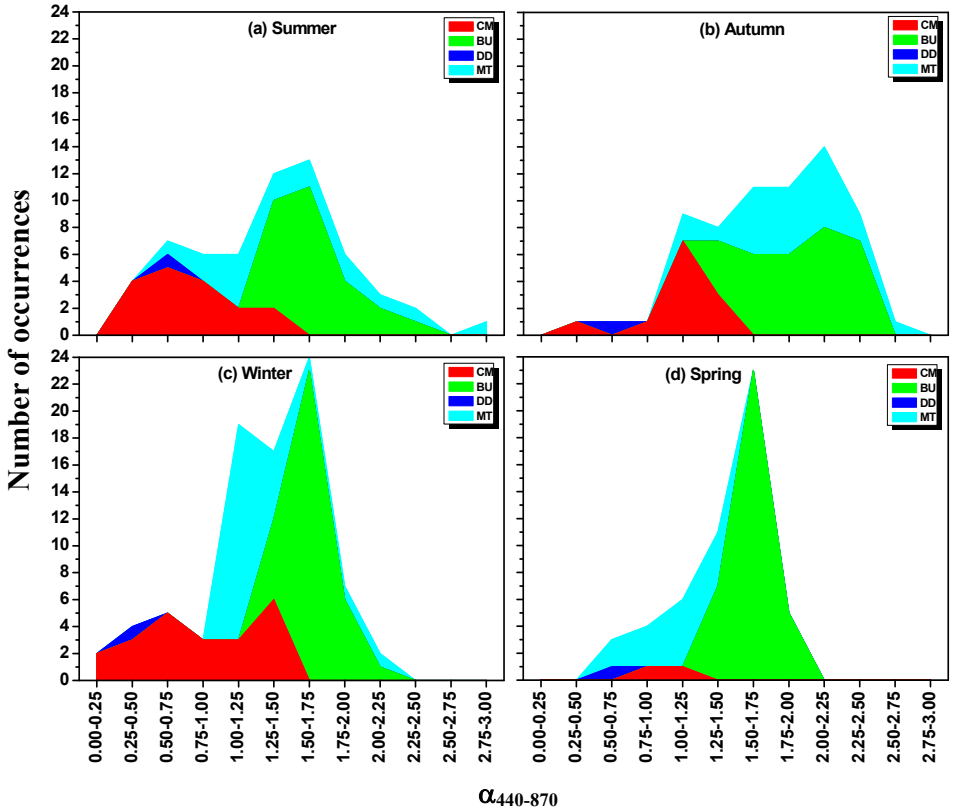

Fig. 6. Same as in Fig. 5, but for the $\alpha_{440\text{-}870}$.

which is further extended for a wide range of $\alpha_{440\text{-}870}$ values (see Fig. 6). These figures are somewhat different from those presented by Kaskaoutis *et al.* (2007a) for four AERONET sites, where, in general, the DD type was dominant for larger AOD_{500}. Dominance of the BU types for high AODs which is similar with the present study was observed over regions affected by biomass burning or urban/industrial pollution (i.e., Alta Floresta and Ispra). Moreover, the discrimination between coarse-mode (sea-salt and desert dust) and fine-mode (biomass burning, urban-industrial pollution) aerosols over the four AERONET sites was obvious using the $\alpha_{440\text{-}870}$ frequency distributions, in contrast to the present study. Therefore, it is concluded that the AOD_{500} or $\alpha_{440\text{-}870}$ values alone cannot identify any aerosol type, except few cases, due to their similar and broad distributions.

Optical Properties of Different Aerosol Types

With the conclusion from the previous section, that the optical properties of aerosols alone cannot provide information about the aerosol types. Indeed, further investigation is required/carried to obtain the information for determining the size and type of aerosol which has been achieved with the computation of spectral curvature a_2 using optical parameters (AOD and α). The mean seasonal values of AOD_{500}, $\alpha_{440\text{-}870}$, and a_2 are given in Table 2 for each aerosol type for the study period over Skukuza. Fig. 7 shows the correlation plot of the spectral coefficient a_2 (curvature in the polynomial fit) against AOD_{500} for the four dominant aerosol types depending on seasons. The correlation between a_2 and AOD_{500} provides information on the atmospheric conditions under which α is independent from wavelength, so the spectral variation of AOD can be accurately described by the simple Ångström formula (Ångström, 1964). The data lying on or near the $a_2 = 0$ line (without curvature) belong to the unimodal size distribution or to bimodal distribution. Near to zero a_2 values can also be caused by a unimodal coarse-mode size distribution, i.e., sea-salt and desert dust dominated (Eck et al., 1999). Negative a_2 values (fine-mode aerosols) are depicted, unexpectedly, for the CM type and correspond to observations associated with larger errors in the a_2 retrievals caused by uncertainties in the polynomial fit under low turbid conditions (Kaskaoutis *et al.*, 2006, 2007a). Furthermore, some positive a_2 values are presented for the BU aerosol type, thus showing that the initial fine-mode aerosols have been modified by coagulation, condensation and gas-to-particle conversion resulting in greater size and less negative or even positive a_2 values (Schuster *et al.*, 2006).

For low turbidity conditions ($AOD_{500} < 0.1$), the coefficient a_2 presents positive values during summer, autumn and winter seasons and negligible in spring. This further reduces as AOD_{500} increases in all the seasons. These high positive values at low AOD are likely due to large uncertainty in computed a_2 for these cases, due to AOD uncertainty of ~0.01. It is interested to note the smaller fraction of positive a_2 values of MT in summer and autumn, highlighting the great fraction of fine-mode particles in its component; whereas, in winter and spring the majority of MT cases correspond to positive a_2. It is concluded that the different aerosol types are rather difficult to be distinguished based on the a_2 values, in contrast to the results in the study by Kaskaoutis *et al.* (2007a) and Kalapureddy *et al.* (2009). However, these researchers investigated the aerosol properties in different environments, where the aerosol types were clearly distinguishable. This is not the case in the present study focused over Skukuza where aerosols from different origins are mixed. So, except CM, DD and some portion of BU (at higher AODs), the other types are still unable to be discriminated unambiguously. It is also note that for low AOD_{500} (< 0.1), there is a wide variability in a_2 values (both positive and negative), thus implying large curvature which increases the uncertainties in the polynomial fit dramatically as well as the errors in the a_2 values. In contrast, a_2 tends to zero for high AOD_{500} indicating small curvature for coarse-mode aerosols and insignificant wavelength dependence of α, which is consistent with

Table 2. Seasonal mean values of AOD_{500}, $\alpha_{440\text{-}870}$ and a_2 for each aerosol type over Skukuza during December 2005–November 2006.

Aerosol Type	Season	AOD_{500}	$\alpha_{440\text{-}870}$	a_2
CM	Summer	0.04 ± 0.01	0.76 ± 0.38	0.51 ± 0.23
	Autumn	0.04 ± 0.02	1.10 ± 0.26	0.72 ± 0.49
	Winter	0.05 ± 0.01	0.88 ± 0.42	0.54 ± 0.36
	Spring	0.04 ± 0.01	1.04 ± 0.23	0.75 ± 0.15
DD	Summer	0.16 ± 0.08	0.68 ± 0.28	0.49 ± 0.24
	Autumn	0.22 ± 0.12	0.69 ± 0.26	0.38 ± 0.19
	Winter	0.19 ± 0.08	0.45 ± 0.19	0.56 ± 0.31
	Spring	0.20 ± 0.11	0.67 ± 0.32	0.57 ± 0.28
BU	Summer	0.22 ± 0.11	1.66 ± 0.27	–0.13 ± 0.25
	Autumn	0.22 ± 0.11	1.93 ± 0.34	–0.17 ± 0.26
	Winter	0.22 ± 0.07	1.66 ± 0.14	0.10 ± 0.22
	Spring	0.32 ± 0.12	1.62 ± 0.13	0.07 ± 0.18
MT	Summer	0.08 ± 0.06	1.50 ± 0.64	–0.08 ± 0.53
	Autumn	0.07 ± 0.02	1.87 ± 0.36	0.09 ± 0.41
	Winter	0.13 ± 0.07	1.28 ± 0.26	0.40 ± 0.23
	Spring	0.15 ± 0.07	1.09 ± 0.21	0.40 ± 0.21

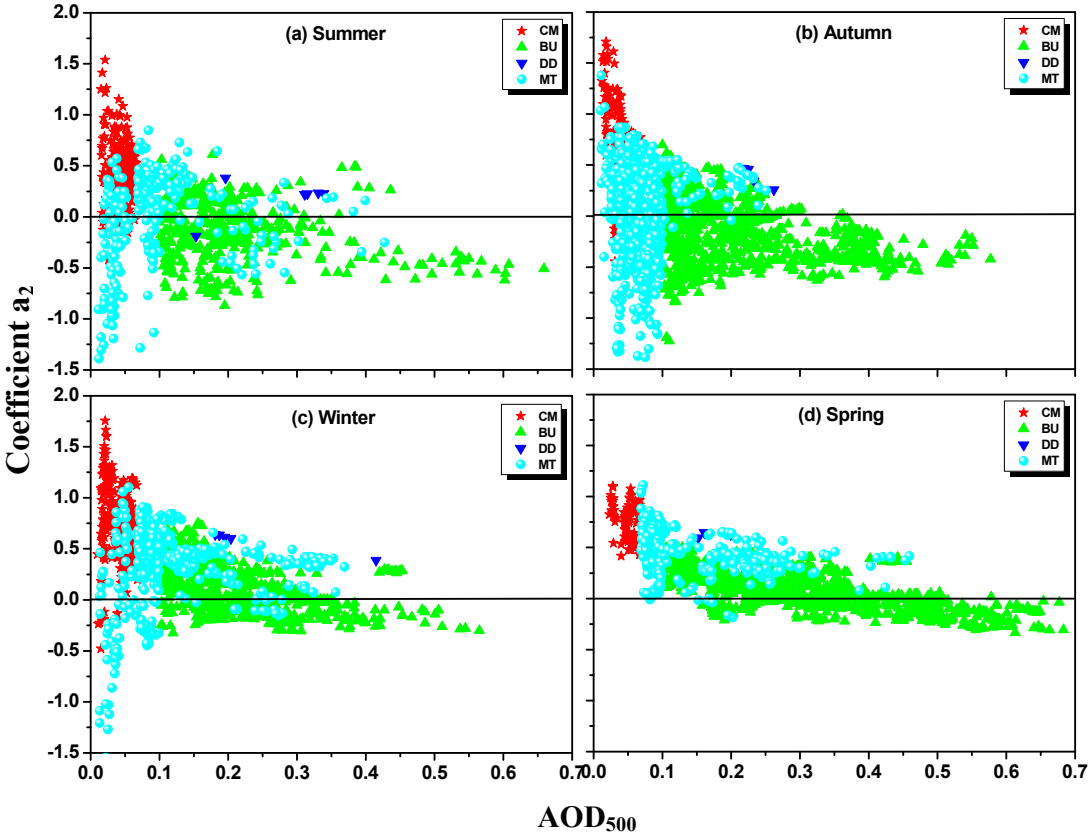

Fig. 7. Seasonal correlations between coefficient a_2 and AOD_{500} for each aerosol type over Skukuza.

those studies reported by several researchers over different urban and oceanic environments (Kaskaoutis and Kambezidis, 2006; Kaskaoutis *et al.*, 2009; Kalapureddy *et al.*, 2009).

Fig. 8 is drawn for further aid in a clear discrimination of the aerosol types, especially DD, which is confined to lower $\alpha_{440\text{-}870}$ values. In general, for a specific value of $\alpha_{440\text{-}870}$, a great spread of a_2 values occur even belonging to different aerosol types (Fig. 8). This is in agreement with the findings of Schuster *et al.* (2006), who showed that different size distributions with the same α can produce large differences in curvature. It is verified that the curvature alone is not enough for describing the aerosol particle size and identifying the types of aerosol, as stated elsewhere (e.g., Eck *et al.*, 1999; Kumar *et al.*, 2013b). Yet it is possible to better discriminate between the different aerosol types by plotting $\alpha_{440\text{-}870}$ versus a_2. However, over Skukuza the optical characteristics of the different aerosol types are not as distinguishable as those presented by Eck *et al.* (1999) and Kaskaoutis *et al.* (2007a). The main difference in the present study is the CM aerosol type, which presents quite different optical characteristics (high $\alpha_{440\text{-}870}$, large negative a_1 and a significant fraction of negative a_2 values) over Skukuza as compared to those over the Solar Village reported in the works of Kaskaoutis *et al.* (2007a). Thus the $\alpha_{440\text{-}870}$ and a_2 values of the CM conditions over the measurement site are similar to those for BU aerosols. Further it is noticed that there is an increasing trend in a_2 values with $\alpha_{440\text{-}870}$ for aerosols dominated by large particles (DD), while opposite exists for aerosols with a large fine fraction (BU).

Classification of Aerosol Types

The aerosol modification processes shown by a graphical scheme based on Gobbi *et al.* (2007) described in one of the sub-sections of previous section over Skukuza are discussed for the study period (Fig. 9), and on seasonal basis (Fig. 10) by representing their AOD_{500} by different colors with increasing value of turbidity. Several key features are obvious from Fig. 9. It is seen that some of the data points at low AOD values ($0.2 > AOD > 0.1$) do fall outside the classification scheme and these may be associated with the larger errors in α, dα estimation and uncertainties while measuring AOD. The scatter plot shows that high AOD values are mainly clustering at the high $\alpha > 1.4$ are associated with fine-mode aerosols (negative dα), and large $\eta > 70\%$ ($R_f < 0.12$ μm) values. However, we notice few cases associated with low AOD (< 0.2), $\alpha < 0.6$ and high $R_f > 0.2$ μm and several cases where moderate-to-high AODs are associated with low $\alpha < 1.0$ and $\eta < 50\%$ values suggesting the presence of coarse-mode particles. The data shown in Fig. 9 also suggest that changes in AOD are mostly associated with the increased concentration of fine-mode particles.

For better understanding the aerosol optical properties, types and modification conditions observed during the year, we have plotted the data on seasonal basis and are shown in Figs. 10(a)–10(d). These figures show unmistakable differences regarding the aerosol types and their modification

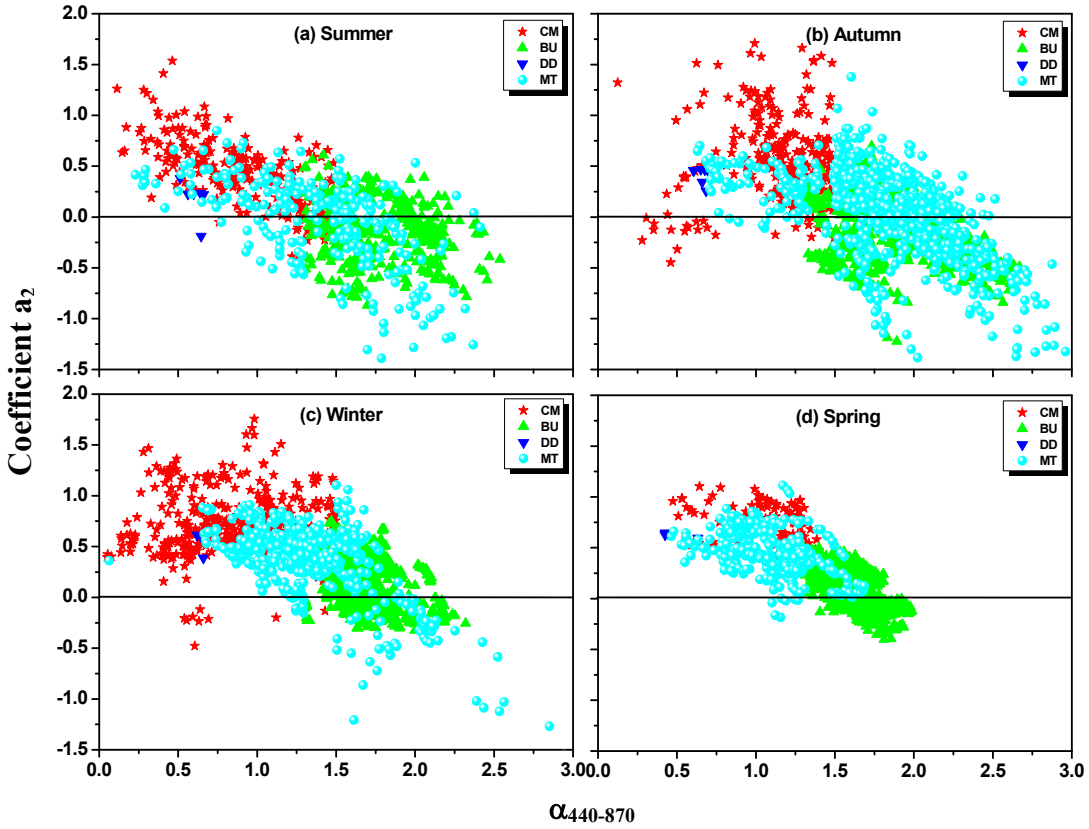

Fig. 8. Same as in Fig. 7, but against $\alpha_{440\text{-}870}$.

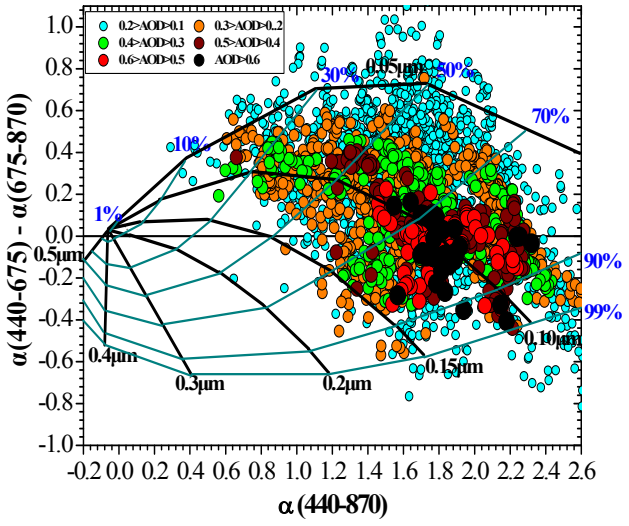

Fig. 9. Ångström exponent difference, dα = α (440–675 nm) – α (675–870 nm), as a function of α (440–870 nm) and AOD_{500} (color-sized scale) over Skukuza, for bimodal and log-normal size distribution. The black lines indicate the fixed effective radius (R_f) of the fine-mode and the dark cyan lines for a fixed fraction (η) of fine-mode to the AOD at 675 nm. Increase of the circle symbols denotes increase in AOD.

processes during the four different climatic periods over Skukuza. As shown in Fig. 10(a), the proportion of large particles during summer shows that few data points having the smaller α (< 1.0) associated with the low AOD (< 0.2) cases show dα values close to zero or positive and η < 50%, suggest the influence of transported mineral dust over the region. Dust transported downwind from source regions varies seasonally. This transport is driven by the latitudinal shift of the Intertropical Front which corresponds to the convergence zone between the northern winds, called the Harmattan and the monsoon winds coming from the South (Basart *et al.*, 2009). In addition to large mineral particles, Skukuza presents cases with mixed AODs (upto 1.5) exhibit larger α (~1.5) values and large negative dα values (> –0.2) that corresponds to a wide range of η (> 70%) and R_f ~0.13 µm. This is due to the well-known presence of biomass burning aerosols composed of fine aerosols originating from anthropogenic activities (Ogunjobi *et al.*, 2008) and associated to urban-industrial pollution aerosols from local and regional activities. The more negative dα with increasing AOD is an indication of fine-mode dominance under high AODs, as also observed over biomass burning regions by Eck *et al.* (2001) and Basart *et al.* (2009). As can be seen from Fig. 10(b), the autumn data (AOD_{500}, α, and dα) exhibits the largest variability in values suggesting diversity in the dominant aerosol types and a mixture of both fine- and coarse-mode particles. For the higher AOD, the majority of data points lie in between (R_f) 0.07 and 0.15 µm lines having larger values of η (> 70%), revealing abundance of fine particle and it is likely the result of secondary aerosol formation through gas-to-particle conversion due to increasing solar radiation (Sinha *et al.*, 2012).

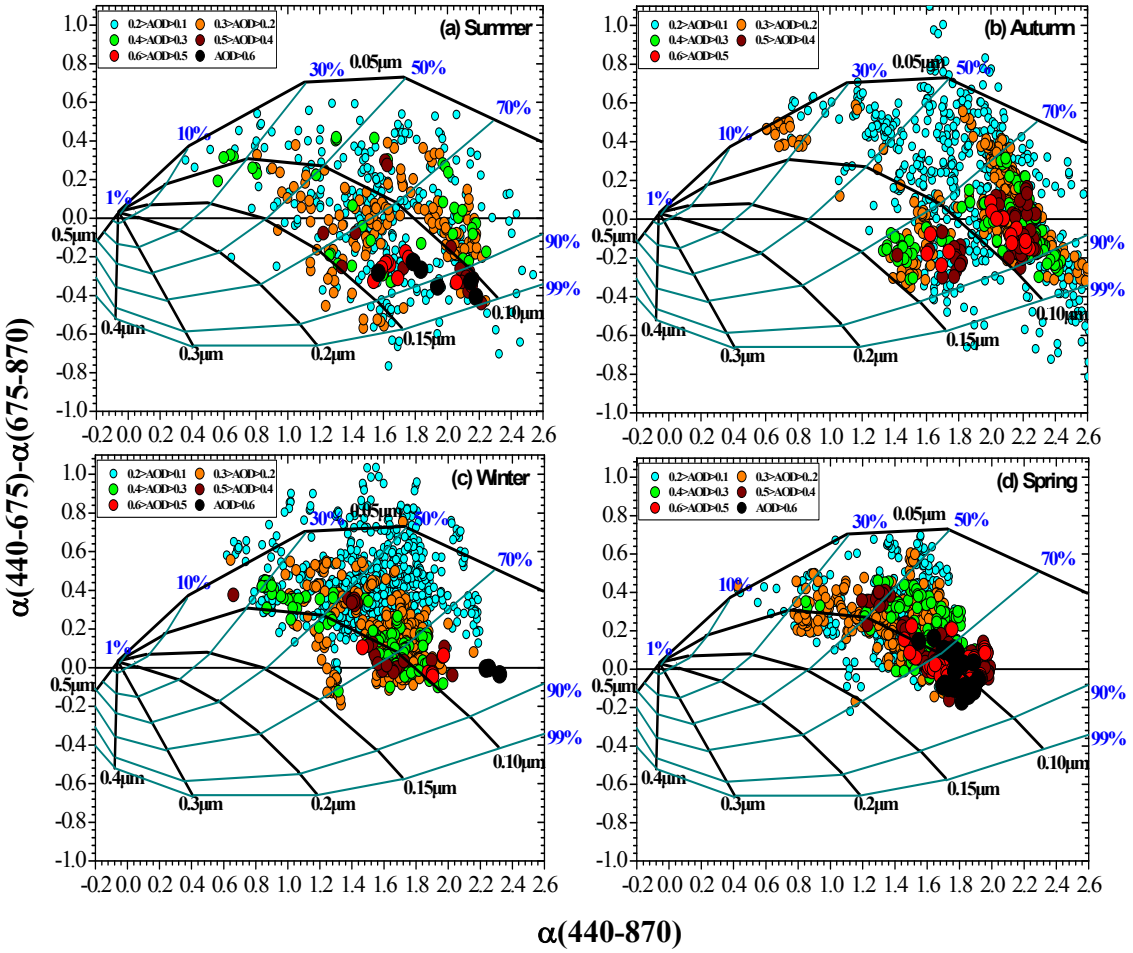

Fig. 10. Same as Fig. 9, but for the four representative seasons.

The α vs. dα plot during winter (Fig. 10(c)) strongly differs from those obtained during other seasons with most of the points lie outside the classification scheme and the main difference being a shift towards the lower α (< 1.0) values with η < 50%; thereby suggesting a dominance of aerosols of coarse-mode. The cases having AOD < 0.1 are associated with large negative dα (> –0.4) values with η > 70% (R_f > 0.2) and may correspond to cases with dilution of the larger particles after rain washout. This R_f value is larger than those found in spring and autumn, suggesting water uptake and increase in size of the water-soluble aerosols due to humidification processes (see Gobbi *et al.*, 2007) as the RH is more over Skukuza during this season. In the spring season (Fig. 10(d)), nearly all the points are within the classification scheme. Increasing AOD shows a shift to larger α values (1.4–1.8) and large negative dα ~–0.3 with η values > 60% suggest the dominance of fine-mode. The data clearly demonstrates that majority of the aerosols in the turbid atmosphere are fine-mode, mainly caused by local anthropogenic pollution or biomass burning, since forest fires are also more frequent in this season due to hot and dry atmospheric conditions apart from agricultural burning. It is also noticed from the Fig. 10(d) that all the points in this season lie close to R_f values ~0.10 µm. The positive dα values indicates that these aerosols are of bimodal distribution having a large coarse-mode fraction between 30% and 50%, whereas, the dα values near to zero represents the lesser dominance of coarse-mode particles relative to fine-mode with η values 50%–70%. As seen in Fig. 10, even though several conclusions regarding the aerosol characteristics over Skukuza are apparent, a large scatter in the data does lead to visual uncertainties.

SUMMARY AND CONCLUSIONS

The characterization of the optical properties of the atmospheric aerosols over Skukuza, as well as their seasonal heterogeneities attributed to the different sources and long-range transport, is of great importance in identifying the dominant aerosol types and assessing their radiative impacts. The present study is carried out mainly focused on the classification and identification of different aerosol types over Skukuza, South Africa to obtain information in determining the aerosol particle size and type using Sunphotometer observations. The results showed a large temporal variation of the examined aerosol properties (AOD_{500}, $\alpha_{440\text{-}870}$, and a_2) over Skukuza strongly affected by the continents, the outflow of pollutants, relative humidity and the mixing processes (e.g., coagulation, humidification) in the rural atmosphere as it has been already reported by

the same authors in their recent works.

The spectral AODs were found to exhibit steep decrease with increase in wavelength and vice-versa, with high values (0.30 ± 0.14) in spring and very low values (0.13 ± 0.11) in autumn season, indicative of dominant presence of fine-mode particles relative to coarse-mode. The analysis of the seasonal data suggest the presence of fine-mode aerosols under turbid atmospheres in spring and winter, the concurrent presence of fine (biomass burning) and coarse (dust) in summer and the significant influence of sea-salt mixed with dust aerosols in autumn. Using the relationship between AOD_{500} and $\alpha_{440\text{-}870}$, four aerosol types were identified over Skukuza region in order to represent different atmospheric conditions (i.e., biomass burning/urban-industrial (BU), clean maritime (CM) and desert dust (DD) aerosols). The cases, which do not belong to any of the above types, are characterized as mixed (undetermined) type (MT) aerosols. The $AOD_{500}/\alpha_{440\text{-}870}$ correlation (contour density) plots over Skukuza revealed the existence of different aerosol types on certain days, months and seasons in contrast to the dominant scenario of a mixed aerosol type in the atmospheric column over this area. The correlation showed that the main aerosol type (BU) over the region corresponded to the (AOD_{500}, $\alpha_{440\text{-}870}$) pair of (0.3, 1.6). The annual frequencies of occurrence of different aerosol types are found to vary strongly with season and month. Thus the higher occurrence of BU (67.31%) aerosols in spring; the predominance of CM and MT conditions was identified in all the seasons with the more occurrence of CM aerosols (28.33%) in summer, while the DD (1.67%) aerosols were mainly found, although rare, in summer period. The CM conditions were nearly absent, while quite interesting was the higher fraction of mixed aerosols (MT), which was dominant during autumn and spring seasons.

The investigation was extended by performing the simple use of the AOD and Ångström exponent data used in deriving the curvature (a_2) showed to obtain information for determining the aerosol-particle size and type of the aerosol. The analysis showed that the inclusion of the curvature (polynomial fit of lnAOD with respect to lnλ) did not significantly improve the aerosol type discrimination over Skukuza. This is attributed to the mixed aerosol field over the region, since particles of different origins and sectors can be present in the atmospheric column. The results of our study confirm the large variability of aerosol optical properties with space and time.

In the present work, we have also provided a graphical framework introduced in Gobbi *et al.* (2007), to classify different aerosol types based on AERONET Sunphotometer data. It is clear from that during summer, dα values close to zero or positive with the low AOD (< 0.2) associated with the smaller α (< 1.0) and η < 50%, suggest the influence of transported mineral dust (coarse) over the region. Whereas in spring, the data clearly demonstrates that an extremely large fraction of fine-mode aerosols in turbid atmosphere, mainly caused by local anthropogenic pollution or biomass aerosol transported from forest fires. This was the most exciting findings in the present work, which differentiates the aerosol characteristics over Skukuza during the study period. Overall, the above classification scheme provides an additional, versatile tool to characterize aerosol properties as well as to explore the information on aerosol-particle size for different aerosol types and aerosol-cloud border region by means of easily accessible, direct Sunphotometric observations.

ACKNOWLEDGEMENTS

The authors extremely thank the University of KwaZulu-Natal (UKZN), South Africa and Nanjing University of Information Science and Technology (NUIST), China for providing financial assistance and necessary infrastructural facilities to carry out this present work. This work partly supported by the National Research Foundation (NRF-South Africa) bi-lateral research grants (UID: 73449 and 78663). Authors are indebted to the AERONET group of NASA, USA for their efforts in making the data available for sun/sky radiometers in the website http://aeronet.gsfc.nasa.gov/. We gratefully acknowledge Prof. Stuart J. Piketh and Prof. B.N. Holben (PIs of Skukuza site) and their staff effort in establishing and maintaining AERONET site related to this investigation. Thanks are owed to South African Weather Services (SAWS) for providing meteorological data. One of the authors KRK thanks Dr. Dimitris G. Kaskaoutis, and Dr. Punaram Sinha, for their kind cooperation in teaching the aerosol classification scheme. The other author RRR acknowledges UGC, India for providing faculty fellowship under UGC-BSR scheme. Thanks are also due to Prof. Neng-Huei (George) Lin, Editor of the journal and the two anonymous reviewers for their critical comments and insightful suggestions which helped to improve the clarity and scientific content of the original article.

REFERENCES

Ångström, A. (1964). The Parameters of Atmospheric Turbidity. *Tellus* 16: 64–75.

Basart, S., Perez, C., Cuevas, E., Baldasano, J.M. and Gobbi, G.P. (2009). Aerosol Characterization in Northern Africa, Northeastern Atlantic, Mediterranenean Basin and Middle East from Direct-sun AERONET Observations. *Atmos. Chem. Phys.* 9: 8265–8282.

Cachoro, V.E., Vergaz, R. and de Frutos, A.M. (2001). A Quantitative Comparison of α-Å Turbidity Parameter Retrieved in Different Spectral Ranges Based on Spectroradiometer Solar Radiation Measurements. *Atmos. Environ.* 5: 5117–5124.

Day, D.E. and Malm, W.C. (2001). Aerosol Light Scattering Measurements as a Function of Relative Humidity: A Comparison between Measurements Made at Three Different Sites. *Atmos. Environ.* 35: 5169–5176.

Dubovik, O., Holben, B.N., Eck, T.F., Smirnov, A., Kaufman, Y.J., King, M.D., Tanre, D. and Slutsker, I. (2002). Variability of Absorption and Optical Properties of Key Aerosol Types Observed in Worldwide Locations. *J. Atmos. Sci.* 59590–59608.

Eck, T.F., Holben, B.N., Reid, J.S., Dubovik, O., Smirnov, A., O'Neill, N.T., Slutsker, I. and Kinne, S. (1999).

Wavelength Dependence of the Optical Depth of Biomass Burning, Urban, and Desert Dust Aerosols. *J. Geophys. Res.* 104: 31333–31349.

Eck, T.F., Holben, B.N., Dubovik, O., Smirnov, A., Slutsker, I., Lobert, J.M. and Ramanathan, V. (2001). Column-integrated Aerosol Optical Properties over the Maldives during the Northeast Monsoon for 1998–2000. *J. Geophys. Res.* 106: 28555–28566.

Eck, T.F., Holben, B.N., Ward, D.E., Mukelabai, M.M., Dubovik, O., Smirnov, A., Schafer, J.S., Hsu, N.C., Piketh, S.J., Queface, A., Le Roux, J., Swap, R.J. and Slutsker, I. (2003a). Variability of Biomass Burning Aerosol Optical Characteristics in Southern Africa during the SAFARI 2000 Dry Season Campaign and a Comparison of Single Scattering Aldebo Estimates from Radiometric Measurements. *J. Geophys. Res.* 108, doi: 10.1029/2002 JD002321.

Eck, T.F., Holben, B.N., Reid, J.S., O'Neill, N.T., Schafer, J.S., Dubovik, O., Smirnov, A., Amaze, M.A. and Arturo, P. (2003b). High Aerosol Optical Depth Biomass Burning Events: A Comparison of Optical Properties for Different Source Regions. *Geophys. Res. Lett.* 30, doi: 10.1029/ 2003GL017861.

Eck, T.F., Holben, B.N., Dubovik, O., Smirnov, A., Glob, P., Chen, H.B., Chatenet, B., Gomes, L., Zhang, X.Y., Stay, S.C., Jig, Q., Giles, D. and Cluster, I. (2005). Columnar Aerosol Optical Properties at AERONET sites in Central Eastern Asia and Aerosol Transport to the Tropical Mid-Pacific. *J. Geophys. Res.* 110: D06202, doi: 10.1029/2004JD005274.

El-Metwally, M., Alfaro, S.C., Abdel, M.W. and Chatenet, B. (2008). Aerosol Characteristics over Urban Cairo: Seasonal Variations as Retrieved from Sun Photometer. *J. Geophys. Res.* 113: D14219: doi: 10.1029/2008JD009834.

Formenti, P., Winkler, H., Fourie, P., Piketh, S.J., Makgopa, B., Helas, G. and Andrea, M.P. (2002). Aerosol Optical Depth over a Remote Semi-arid Region of South Africa from Spectral Measurements of the Daytime Solar Extinction and the Nighttime Stellar Extinction. *Atmos. Res.* 62: 11–32.

Freiman, M.T. and Piketh, S.J. (2003). Air Transport into and out of the Industrial Highveld Region of South Africa. *J. Appl. Meteorol.* 42: 994–1002.

Gerasopoulos, E., Amiridis, V., Kazadzis, S., Kokkalis, P., Eleftheratos, K., Andrea, M.O., Andrea, T.W., El-Askary, H. and Zerefos, C.S. (2011). Three-year Ground Based Measurements of Aerosol Optical Depth over the Eastern Mediterranean: The Urban Environment of Athens. *Atmos. Chem. Phys.* 11: 2145–2159.

Gobbi, G.P., Kaufman, Y.J., Koren, I. and Eck, T.F. (2007). Classification of Aerosol Properties Derived from AERONET Direct Sun Data. *Atmos. Chem. Phys.* 7: 453–458.

Holben, B.N., Eck, T.F., Slutsker, I., Tanré, D., Buis, J.P., Setzer, A., Vermote, E., Reagan, J.A., Kaufman, Y.J., Nakajima, T., Lavenu, F., Jankowiak, I. and Smirnov, A. (1998). AERONET—A Federated Instrument Network and Data Archive for Aerosol Characterization. *Remote Sens. Environ.* 66: 1–16.

Holben, B.N., Tanre, D., Smirnov, A., Eck, T.F., Slutsker, I. *et al.* (2001). An Emerging Ground-based Aerosol Climatology: Aerosol Optical Depth from AERONET. *J. Geophys. Res.* 106: 12067–12097.

Intergovernmental Panel on Climate Change (IPCC) (2007). Climate Change. The Physical Science Basis: Contribution of Working Group I to the Fourth Assessment Report of the Intergovernmental Panel on Climate Change, Chapter 2, 129pp.

Kalapureddy, M.C.R., Kaskaoutis, D.G., Raj, P.E., Devara, P.C.S., Kambezidis, H.D., Kosmopoulos, P.G. and Nastos, P.T. (2009). Identification of Aerosol Type over the Arabian Sea in the Premonsoon Season during the Integrated Campaign for Aerosols, Gases and Radiation Budget (ICARB). *J. Geophys. Res.* 114: D17203, doi: 10.1029/2009JD011826.

Kanike, R.K., Sivakumar, V., Reddy, R.R. and Gopal, K.R. (2012). Latitudinal Variations of Aerosols in the MABL over Bay of Bengal, Proc. of 2012 Annu. IEEE India Conf., Kochi, Kerala, India, December 7–9, ISBN: 978-1-4673-2272-0: 536-539.

Kaskaoutis, D.G. and Kambezidis, H.D. (2006). Investigation on the Wavelength Dependence of the Aerosol Optical Depth in the Athens Area. *Q. J. R. Meteorolog. Soc.* 132: 2217–2234.

Kaskaoutis, D.G., Kambezidis, H.D., Adamopoulos, A.D. and Kassomenos, P.A. (2006). Comparison between Experimental Data and Modeling Estimates of Atmospheric Optical Depth over Athens, Greece. *J. Atmos. Sol. Terr. Phys.* 68: 1167–1178.

Kaskaoutis, D.G. and Kambezidis HD. (2008). Comparison of the Angstrom Parameters Retrieval in Different Spectral Ranges with the Use of Different Techniques. *Meteorol. Atmos. Phys.* 99: 233–246.

Kaskaoutis, D.G., Kambezidis, H.D., Hatzianastassiou, N., Kosmopoulos, P.G. and Badarinath, K.V.S. (2007a). Aerosol Climatology: On the Discrimination of Aerosol Types over four AERONET Sites. *Atmos. Chem. Phys. Discuss.* 7: 6357–6411.

Kaskaoutis, D.G., Kambezidis, H.D., Hatzianastassiou, N., Kosmopoulos, P.G. and Badarinath, K.V.S. (2007b). Aerosol Climatology: Dependence of the Angstrom Exponent on Wavelength over four AERONET Sites. *Atmos. Chem. Phys. Discuss.* 7: 7347–7397.

Kaskaoutis, D.G., Badarinath, K.V.S., Kharol, S.K., Sharma, A.R. and Kambezidis, H.D. (2009). Variations in the Aerosol Optical Properties and Types over the Tropical Urban Site of Hyderabad, India. *J. Geophys. Res.* 114: D22204, doi: 10.1029/2009JD012423.

Kaskaoutis, D.G., Kalapureddy, M.C.R., Moorthy, K.K., Devara, P.C.S., Nastos, P.T., Kosmopoulos, P.G. and Kambezidis, H.D. (2010). Heterogeneity in Pre-monsoon Aerosol Types over the Arabian Sea Deduced from Ship-borne Measurements of Spectral AODs. *Atmos. Chem. Phys.* 10: 4893–4908.

Kaskaoutis, D.G., Kharol, S.K., Sinha, P.R., Singh, R.P., Kambezidis, H.D., Sharma, A.R. and Badarinath, K.V.S. (2011). Extremely Large Anthropogenic-aerosol Contribution to Total Aerosol Load over the Bay of

Bengal during Winter Season. *Atmos. Chem. Phys.* 11: 7097–7117.

Kim, D.H., Sohn, B.J., Nakajima, T., Takamura, T., Choi, B.C. and Yoon, S.C. (2004). Aerosol Optical Properties over East Asia Determined From Ground-Based Sky Radiation Measurements. *J. Geophys. Res.* 109: D02209, doi: 10.1029/2003JD003387.

King, M.D. and Byrne, D.M. (1976). A Method for Inferring Total Ozone Content from Spectral Variation of Total Optical Depth Obtained with a Solar Radiometer. *J. Atmos. Sci*. 33: 2242–2251.

Kumar, K.R., Narasimhulu, K., Reddy, R.R., Gopal, K.R., Reddy, L.S.S., Balakrishnaiah, G., Moorthy, K.K. and Babu, S.S. (2009). Temporal and Spectral Characteristics of Aerosol Optical Depths in a Semi-arid Region of Southern India. *Sci. Total Environ.* 407: 2673–2688.

Kumar, K.R., Adesina, A.J. and Sivakumar, V. (2013a). Aerosol Radiative Forcing from Spectral Solar Attenuation Measurements due to Aerosol Loading Using AERONET over Pretoria in South Africa, Proc. 2013 IEEE Annu. Int. Conf. on Emerg. Res. Areas: Int. Conf. on Microelec., Communi., and Renew., Energ., Kanjirappally, Kerala, India, June 4–6, ISBN: 978-1-4673-5149-2: 1-4.

Kumar, K.R., Sivakumar, V., Reddy, R.R.., Gopal, K.R., Adesina, A.J. (2013b). Inferring Wavelength Dependence of AOD and Ångström Exponent over a Sub-tropical Station in South Africa Using AERONET Data: Influence of Meteorology, Long-range Transport and Curvature Effect. *Sci. Total Environ* 461–462: 397–408.

Masmoudi, M., Chaabane, M., Tanré, D., Gouloup, P., Blarel, L., Elleuch, F. (2003). Spatial and Temporal Variability of Aerosol: Size Distribution and Optical Properties. *Atmos. Res.* 66: 1–19.

Moorthy, K.K., Babu, S.S. and Satheesh, S.K. (2005). Aerosol Characteristics and Radiative Impacts over the Arabian Sea during the Intermonsoon Season: Results from ARMEX Field Campaign. *J. Atmos. Sci.* 62: 192–206.

Morgan, M.G., Adams, P.J. and Keith, D.W. (2006). Elicitation of Expert Judgments of Aerosol Forcing. *Clim. Change* 75: 195–214.

Ogunjobi, K.O., He, Z., Kim, K.W. and Kim, Y.J. (2004). Aerosol Optical Depth during Episodes of Asian Dust Storms and Biomass Burning at Kwangju, South Korea. *Atmos. Environ.* 38: 1313–1323.

Ogunjobi, K.O., He, Z. and Simmer, C. (2008). Spectral Aerosol Optical Properties from AERONET Sun-photometric Measurements over West Africa. *Atmos. Res.* 88: 89–107.

Pace, G., di Sarra, A., Meloni, D., Piacentino, S. and Chamard, P. (2006). Aerosol Optical Properties at Lambeduca (Central Mediterranean), 1. Influence of Transport and Identification of Different Aerosol Types. *Atmos. Chem. Phys.* 6: 697–713.

Pedros, R., Martinez-Lozano, J.A., Utrillas, M.P., Gomez-Amo, J.L., Tena, F. (2003). Column-integrated Aerosol, Optical Properties from Ground-based Spectroradiometer Measurements at Barrax (Spain) during the Digital Airborne Imaging Spectrometer Experiment (DAISEX) Campaigns. *J. Geophys. Res.* 108: 4571–4587.

Penner, J.E., Charlson, R.J., Hales, J.M., Laulainen, N.S., Leifer, R., Novakov, T., Orgen, J., Radke, L.F., Schwartz, S.E. and Travis, L. (1994). Quantifying and Minimizing Uncertainty of Climate Forcing by Anthropogenic Aerosols. *Bull. Am. Meteorol. Soc.* 75: 375–400.

Piketh, S.J., Annegarn, H.J. and Tyson, P.D. (1999). Lower Tropospheric Aerosol Loadings over South Africa: The Relative Contribution of Aeolian Dust, Industrial Emissions, and Biomass Burning. *J. Geophys. Res.* 104: 1597–1607.

Queface, A.J., Piketh, S.J., Eck, T.F., Tsay, S.C. and Mavume, A.F. (2011). Climatology of Aerosol Optical Properties in Southern Africa. *Atmos. Environ.* 45: 2910–2921.

Rana, S., Kant, Y. and Dadhwal, V.K. (2009).Diurnal and Seasonal Variation of Spectral Properties of Aerosols over Dehradun, India. *Aerosol Air Qual. Res*. 9: 32–49.

Reid, J.S., Eck, T.F., Christopher, S.A., Hobbs, P.V. and Holben, B.N. (1999). Use of the Ångström Exponent to Estimate the Variability of Optical and Physical Properties of Aging Smoke Particles in Brazil. *J. Geophys. Res.* 104: 27473–27489.

Schuster, G.L., Dubovik, O. and Holben, B.N. (2006). Angstrom Exponent and Bimodal Aerosol Size Distributions. *J. Geophys. Res.* 111: D07207, doi: 10.1029/2005JD006328.

Seinfeld, J.H. and Pandis, S.N. (2006). *Atmospheric Chemistry and Physics: From Air Pollution to Climate Change* (Second Edition), John Wiley and Sons, Inc., Hoboken, New Jersey.

Sinha, P.R., Kaskaoutis, D.G., Manchanda, R.K. and Sreenivas, S. (2012). Characteristics of Aerosols over Hyderabad in Southern Peninsular India: Synergy in the Classification Techniques. *Ann. Geophys.* 30: 1393–1410.

Sivakumar, V., Tesfaye, M., Alemu, W., Sharma, A., Bollig, C. and Mengistu, G. (2010). Aerosol Measurements over South Africa Using Satellite, Sun-photometer and LIDAR. *Adv. Geosci.* 16: 253–262.

Sivertsen, B., Matale, C. and Pereiira, L.M.R. (1995). *Sulphur Emissions and Transfrontier, Air Pollution in Southern Africa*, Report No. 35, SADC Environment and Land Management Sector Coordination Unit, Maseru.

Smirnov, A., Holben, B.N., Eck, T.F., Dubovik, O. and Slutsker, I. (2000). Cloud Screening and Quality Control Algorithms for the AERONET Data Base. *Rem. Sens. Environ.* 73: 337–349.

Smirnov, A., Holben, B.N., Dubovik, O., O'Neill, N.T., Eck, T.F., Westphal, D.L., Goroth, A.K., Pietras, and C, Slutsker, I. (2002a). Atmospheric Aerosol Optical Properties in the Persian Gulf. *J. Atmos. Sci.* 59: 620–634.

Smirnov, A., Holben, B.N., Kaufman, Y.J., Dubovik, O., Eck, T.F., Slutsker, I., Pietras, C. and Halthore, R.L. (2002b). Optical Properties of Atmospheric Aerosol in Maritime Environments. *J. Atmos. Sci.* 59: 501–523.

Srivastava, A.K., Tripathi, S.N., Dey, S., Kanawade, and V.P., Tiwari, S. (2012). Inferring Aerosol types over the Indo-Gangetic Basin from Ground Based Sunphotometer

Measurements. *Atmos. Res.* 109: 64–75.

Tesfaye, M., Sivakumar, V., Botai, J. and Tsidu, G.M. (2011). Aerosol Climatology over South Africa Based on 10 Years of Multiangle Imaging Spectroradiometer (MISR) Data. *J. Geophys. Res.* 116: D20216, doi: 10.1029/2011JD016023.

Vijayakumar, K., Devara, P.C.S. and Simha, C.P. (2012). Aerosol Features during Drought and Normal Monsoon Years: A Study Undertaken with Multi-platform Measurements over a Tropical Urban Site. *Aerosol Air Qual. Res*. 12: 1444–1458.

Received for review, March 22, 2013
Accepted, August 8, 2013